A&A 633, L9 (2020)
https://doi.org/10.1051/0004-6361/201937140

Astronomy & Astrophysics

LETTER TO THE EDITOR

Traits for chemical evolution in solar twins

Trends of neutron-capture elements with stellar age*

Paula Jofré[1], Holly Jackson[2], and Marcelo Tucci Maia[1]

[1] Núcleo de Astronomía, Universidad Diego Portales, Ejército 441, Santiago, Chile
e-mail: paula.jofre@mail.udp.cl
[2] Department of Electrical Engineering and Computer Science, Massachusetts Institute of Technology, 50 Vassar Street, Cambridge, MA 02139, USA

Received 19 November 2019 / Accepted 5 December 2019

ABSTRACT

The physical processes driving chemical evolution in the Milky Way can be probed using the distribution of abundances in low-mass FGK type stars in space phase at different times. During their final stages of evolution, stars experience nucleosynthesis several times, each at different timescales and producing different chemical elements. Finding abundance ratios that have simple variations across cosmic times therefore remains a challenge. Using the sample of 80 solar twins for which ages and abundances of 30 elements have been measured with high precision, we searched for all possible abundance ratio combinations that show linear trends with age. We found 55 such ratios, all combining an *n*-capture element and another element produced by different nucleosynthesis channels. We recovered the ratios of [Y/Mg], [Ba/Mg], and [Al/Y] that have been reported previously in the literature, and found that [C/Ba] depends most strongly on age, with a slope of 0.049 ± 0.003 dex Gyr^{-1}. This imposes constraints on the magnitude of the time dependency of abundance ratios in solar twins. Our results suggest that *s*-process elements, in lieu of Fe, should be used as a reference for constraining chemical evolution models of the solar neighbourhood. Our study illustrates that a wide variety of chemical elements measured in high-resolution spectra is key to meeting the current challenges in understanding the formation and evolution of our Galaxy.

Key words. stars: abundances – solar neighborhood

1. Introduction

Chemical abundances of FGK low-mass stars have shown to be powerful tracers of the Milky Way evolution because we assume that the chemical composition of the birthplaces of these stars is recorded in their photosphere. Because chemical composition evolves from one stellar generation to the next, it is possible to reconstruct the different physical processes that shaped the Milky Way across cosmic times by combining this information with stellar age and phase-space (Freeman & Bland-Hawthorn 2002).

The evolution of chemistry in the Milky Way is mainly due to stellar nucleosynthesis (Nomoto et al. 2013; Karakas & Lugaro 2016). Newly synthesized metals are returned to the interstellar medium and are recycled in new stars, and their elemental abundances thereby increase with time (da Silva et al. 2012). It is therefore commonly assumed that the chemical composition of stars that is imprinted in their atmospheres remains unchanged in a stellar lifetime, but it evolves in time through inheritance between stellar generations (Jofré et al. 2017). Each chemical abundance measured from a stellar spectrum can therefore be understood as a trait for reconstructing the chemical evolution of the Galaxy.

Not all chemical elements are informative traits for chemical evolution studies because in reality, some of them may change during a stellar lifetime. Inner processes in stellar evolution such diffusion (Dotter et al. 2017) or planet formation or engulfment (Meléndez et al. 2009; Tucci Maia et al. 2019) alter the chemical composition in stars. Other inner mixing processes produced during dredge-up or induced by rotation can alter abundances such as [C/N] or Li (Masseron et al. 2017; Aguilera-Gómez et al. 2018). We have to assume today that a selection of chemical abundances remains approximately intact in FGK main-sequence stars and can be used to trace chemical evolution.

A few years ago, da Silva et al. (2012) studied several traits for chemical evolution studies of solar-type stars. In particular, [Y/Mg], [Sr/Mg], [Y/Zn], and [Sr/Zn] showed a significant trend as a function of age for their entire sample. When they performed a linear fit of [Y/Mg] as a function of stellar age for a sample of nearby solar twins, Nissen (2015) obtained slope of ∼0.04 dex Gyr^{-1} and interpreted this relation using nucleosynthesis arguments: massive stars produced Mg and expelled it into the interstellar medium on a different timescale than intermediate-mass stars reaching the AGB and producing Y. This has motivated discussions about whether abundance ratios can be used as "chemical clocks", in particular if ages are difficult to measure. The exact dependence of [Y/Mg] or [Ba/Mg] on age is still debated, because it seems to further depend on stellar properties such as metallicity (Feltzing et al. 2017;

* The results of the linear fits are only available at the CDS via anonymous ftp to cdsarc.u-strasbg.fr (130.79.128.5) or via http://cdsarc.u-strasbg.fr/viz-bin/cat/J/A+A/633/L9

Skúladóttir et al. 2019; Delgado Mena et al. 2019), but not evolutionary state, at least before the AGB phase (Slumstrup et al. 2017). In addition to [Y/Mg] and [Ba/Mg], [Al/Y] has also shown similar dependences with age (Nissen 2016; Spina et al. 2016), at least for solar twins.

Several other works that benefit from accurate age estimates have studied trends of abundance ratios as a function of age (Bedell et al. 2018; Spina et al. 2018; Delgado Mena et al. 2019; Feuillet et al. 2018, to mention recent works). Most of these analyses have been restricted to using abundance ratios in their classical form, as a function of iron (see Delgado Mena et al. 2019 for exception). Motivated by the fact that the chemical clocks discussed above do not include iron, we searched for other combinations in a sample of 30 elemental abundances. We found 55 relations that are as significant as those mentioned above. This new set of ratios can be used for the same applications as [Y/Mg]. In addition, the ratios can be applied to models of Galaxy evolution and to build stellar phylogenies (Jofré et al. 2017; Jackson et al., in prep.). We report these findings in this Letter.

2. Data and methods

We considered the sample of 80 solar twins (including the Sun) that was analysed by Bedell et al. (2018, and references therein) and Spina et al. (2018). This is the largest sample of solar twins that has been analysed using the differential technique for high-precision estimates of the abundances of 30 elements and stellar ages. The age and abundance data together with the list of stars can be found in these references.

In short, Bedell et al. (2018) and Spina et al. (2018) measured chemical abundances using spectra obtained with the High Accuracy Radial velocity Planet Searcher (HARPS) at La Silla, taken from the public ESO Science Archive Facility. The spectra have very high resolving power (100 000). For multiple observations, the spectra were stacked to achieve a very high signal-to-noise ratio (S/N) of above 200 pix^{-1}. In addition, spectra taken with the Magellan Inamori Kyocera Echelle spectrograph (MIKE) at Las Campanas of slightly lower resolution (65 000–80 000) but equal S/N were used to complement the wavelength ranges that are not covered by HARPS. This allowed the researchers to measure abundances of elements such as oxygen from the O triplet at 770 nm. Stellar parameters and abundances were derived using a 1D local thermal equilibrium (LTE) analysis based on equivalent widths. Stellar ages were estimated using fits to isochrones following the same procedure as described in Spina et al. (2018).

We considered all possible combinations of abundance ratios of all 30 elements and performed a linear regression fit to these ratios as a function of age. Unlike Bedell et al. (2018) and Spina et al. (2018), we considered all stars, including the very old ones that are assumed to be part of the thick disc and might follow a different chemical enrichment history. The regression fit was made using the python 2.7 routine `stats.linregress` from the `scipy` library.

We only considered traits whose linear fit had an absolute slope greater than 0.03 dex Gyr^{-1} and a correlation factor greater than 0.7. Our choice for this threshold for the slope was motivated by the slope of linear fits of abundance ratios as a function of Fe, which is normally lower than 0.03 dex Gyr^{-1}; see Bedell et al. (2018). We were interested in finding relations that are as significant as the [Y/Mg] or [Ba/Mg] relations discussed in the literature, which have a slope greater than 0.03 dex Gyr^{-1}. We note that different fitting techniques, selection of stars, thresholds for the slopes, and correlation coefficients might yield slightly different results and therefore a different final sample of selected traits. The results of the linear fits of all abundance combinations as a function of age are available at the CDS.

3. Results

The linear correlation coefficients for the selected traits are listed in Table 1. The fit is also plotted in Fig. 1 alongside the abundance ratio for each star as a function of age. Each trait is plotted in a different panel and is indicated in the top left corner.

For better interpretation of the results, we have added two boxes with labels and colours in the bottom right corner that help to attribute the chemical element involved in the trait to a nucleosynthesis family. The left-hand side box represents the family of the element in the numerator and the right-hand side box represents the family of the element in the denominator of the abundance ratio. The families were chosen following the classification indicated in Table 2. This classification comes from discussions in Nomoto et al. (2013), except for the neutron-capture family, for which we simply considered the elements analysed by Spina et al. (2018). As extensively discussed in that work (see also Bisterzo et al. 2014; Karakas & Lugaro 2016; Battistini & Bensby 2016), it is difficult to determine how much of these elements is produced by the slow neutron-capture process (s) and how much by the rapid neutron-capture process (r), which each have a different site. We therefore decided to include all elements in the same family here.

We note that Nomoto et al. (2013) did not consider titanium as an α-capture element because the theoretical prediction for this element does not match the observations (Kobayashi et al. 2006). However, observationally, Ti behaves like an α-element, at least in terms of the abundance trends as a function of [Fe/H]. We therefore include it in this family. Carbon belongs to a special family that we call `sa` because carbon has multiple unique formation sites. It can be produced in AGB stars through s-process or from massive stars through α-capture (see Amarsi et al. 2019, for extensive discussions). While other elements are also produced by a variety of channels, the carbon mass production is believed to be significant in all these channels.

We find that all selected traits involve different families. The ratios selected here consider elements in their [X/Fe] form with opposite (increasing vs. decreasing) trends with age. Spina et al. (2018) obtained negative trends of the n-capture elements in their [X/Fe] form as a function of age, and Bedell et al. (2018) obtained both positive and negative slopes for the other elements. The traits found here correspond to abundance ratios of elements that showed a general positive trend in their [X/Fe] vs. age correlation in Bedell et al. (2018).

We further find that the denominator of our selected abundance ratios is always an n-capture element, including the previously studied traits [Mg/Y] and [Mg/Ba]. The slopes in our fits are 0.042 and 0.047 dex Gyr^{-1}, respectively. This agrees well with previous findings (Nissen 2015; Tucci Maia et al. 2016). The n-capture elements selected here are known to receive a contribution of more than 50% from the s-process in the Sun (see Spina et al. 2018, for a discussion on this sample). The percentages were calculated by Bisterzo et al. (2014). Elements with lower percentage in s-process contribution for the solar abundances (e.g. Eu, Sm, or Dy) were not selected to vary enough with age, according the restrictions imposed in this analysis. The trend of [C/Ba] with age has the largest slope in our sample of 0.049 ± 0.003 dex Gyr^{-1}. This places a constraint on the maximum change of abundance ratio with age on this sample of solar metallicity stars.

Table 1. Linear regression fit coefficients.

Trait	Slope (dex Gyr^{-1})	Intercept (dex)	Error (dex Gyr^{-1})	r^2	Trait	Slope (dex Gyr^{-1})	Intercept (dex)	Error (dex Gyr^{-1})	r^2
[CI/YII]	0.043	−0.226	0.304	0.721					
[CI/ZrII]	0.040	−0.228	0.277	0.733	[CI/BaII]	0.049	−0.293	0.255	0.822
[CI/LaII]	0.039	−0.242	0.245	0.762	[CI/CeII]	0.038	−0.252	0.234	0.777
[CI/NdII]	0.035	−0.252	0.248	0.724	[OI/YII]	0.032	−0.171	0.229	0.713
[OI/BaII]	0.037	−0.238	0.240	0.754	[NaI/SrI]	0.039	−0.181	0.267	0.736
[NaI/YII]	0.038	−0.164	0.239	0.765	[NaI/ZrII]	0.035	−0.165	0.212	0.783
[NaI/BaII]	0.043	−0.231	0.187	0.874	[NaI/LaII]	0.034	−0.180	0.195	0.792
[NaI/CeII]	0.033	−0.190	0.177	0.820	[NaI/NdII]	0.030	−0.190	0.185	0.775
[MgI/SrI]	0.043	−0.202	0.281	0.752	[MgI/YII]	0.042	−0.185	0.255	0.776
[MgI/ZrII]	0.039	−0.187	0.232	0.786	[MgI/BaII]	0.047	−0.252	0.201	0.876
[MgI/LaII]	0.037	−0.201	0.221	0.786	[MgI/CeII]	0.037	−0.211	0.204	0.810
[MgI/NdII]	0.034	−0.212	0.212	0.769	[AlI/YII]	0.031	−0.146	0.219	0.725
[AlI/BaII]	0.037	−0.213	0.172	0.854	[SiI/ZrII]	0.032	−0.168	0.235	0.703
[SiI/BaII]	0.040	−0.233	0.219	0.811	[SiI/LaII]	0.030	−0.182	0.211	0.724
[SiI/CeII]	0.030	−0.193	0.205	0.734	[CaI/BaII]	0.033	−0.192	0.179	0.817
[ScI/SrI]	0.038	−0.180	0.274	0.707	[ScI/YII]	0.036	−0.162	0.246	0.737
[ScI/ZrII]	0.034	−0.164	0.223	0.745	[ScI/BaII]	0.042	−0.229	0.204	0.843
[ScI/LaII]	0.032	−0.178	0.221	0.727	[ScI/CeII]	0.032	−0.189	0.200	0.763
[ScII/BaII]	0.035	−0.186	0.153	0.870	[TiI/YII]	0.033	−0.141	0.238	0.705
[TiI/BaII]	0.038	−0.207	0.169	0.865	[TiII/BaII]	0.032	−0.187	0.163	0.834
[MnI/YII]	0.032	−0.160	0.226	0.720	[MnI/BaII]	0.037	−0.227	0.204	0.812
[CoI/BaII]	0.035	−0.224	0.208	0.781	[NiI/SrI]	0.042	−0.225	0.253	0.779
[NiI/YII]	0.041	−0.208	0.226	0.805	[NiI/ZrII]	0.038	−0.210	0.221	0.791
[NiI/BaII]	0.046	−0.275	0.234	0.832	[NiI/LaII]	0.036	−0.224	0.251	0.727
[NiI/CeII]	0.036	−0.234	0.238	0.745	[CuI/SrI]	0.039	−0.211	0.270	0.729
[CuI/YII]	0.038	−0.194	0.243	0.757	[CuI/ZrII]	0.035	−0.196	0.236	0.741
[CuI/BaII]	0.043	−0.261	0.223	0.828	[CuI/LaII]	0.033	−0.210	0.240	0.712
[CuI/CeII]	0.033	−0.221	0.234	0.720	[ZnI/BaII]	0.038	−0.257	0.231	0.773

Notes. The error is the standard error ($\times 10^2$); r^2 is the correlation coefficient.

The final 55 abundance ratios contain 6 ratios with carbon, 17 with α-capture elements, 10 with iron-peak elements, and 22 with odd-Z elements. Among the α-capture, we obtain traits including O, Mg, Si, and Ti. The element S was not selected. Among the iron-peak, we obtain traits including Mn, Co, Ni, and Zn. It is interesting that Fe was not selected because it is the standard element used for abundance ratios. Cr was not selected either. Regarding the odd-Z, we find Na, Al, Sc, and Cu selected, but not V.

In order to investigate the abundance ratios further, we grouped the traits by the different n-capture elements or by the families of the numerator of the abundance ratios. The mean and standard deviation of the slopes for each of the groups are listed in Table 3, where we also indicate the total times a given abundance or family was selected.

Regarding the $n-$capture elements, the largest mean slopes are obtained for Sr and Ba, although the mean slope for Ba has the largest standard deviation. However, there is no relation between the contribution of the solar s-process and the slopes for the age trends when we consider the values adopted by Spina et al. (2018), which were obtained by Bisterzo et al. (2014).

The mean slopes of the different families show that carbon has the largest mean slope, but they all seem to be of comparable magnitudes, especially when we consider their standard deviations. These results are further visualised in Fig. 2, where we plot the mean slope and standard deviation of the mean for each family. The first panel contains all selected n-capture elements, and the second and third panels show the results for Ba and Y because these elements were shown to contribute to ratios of elements in all families. We note that the error bar for Ba and Y in the `sa` family corresponds to the uncertainty of the linear fit (see Table 1 for [C/Ba] and [C/Y]). All family combinations behave similarly, and C systematically yields higher slopes.

4. Discussion

Neutron-capture elements, in particular those produced by the s-process, have been shown to add crucial information in chemical evolution studies (see the recent study of Skúladóttir et al. 2019). Their gradual and slow production as intermediate-mass stars reaches the AGB phase and produces stellar winds that carry the newly synthesised elements into the ISM. This means that new generations of stars that are formed within this environment will inherit a gradual increase of s-process elements. Because the production of s-process depends on the overall metallicity of the progenitor star (Karakas & Lugaro 2016), the enrichment of s-process elements is highly dependent on the local conditions and star formation history of the previous generations.

With this in mind, the relation of [Mg/Y] or [Mg/Ba] as a function of age has been explained with the chemical evolution principle in the literature. It is therefore expected that not only would these two ratios show significant trends as a function of stellar age, but that other ratios involving both α-capture and s-process elements, such as the other 15 cases resulting from our exercise, would show these trends as well. Although C behaves as both an α-capture and n-capture element, we find six traits with a strong dependence of C on a s-process element with age. This suggests that the C contribution to chemical evolution from s-process is lower than from α-capture, at least at solar metallicities. This reasoning might contradict the results of Amarsi et al. (2019), who studied the [C/O] ratio for different stellar

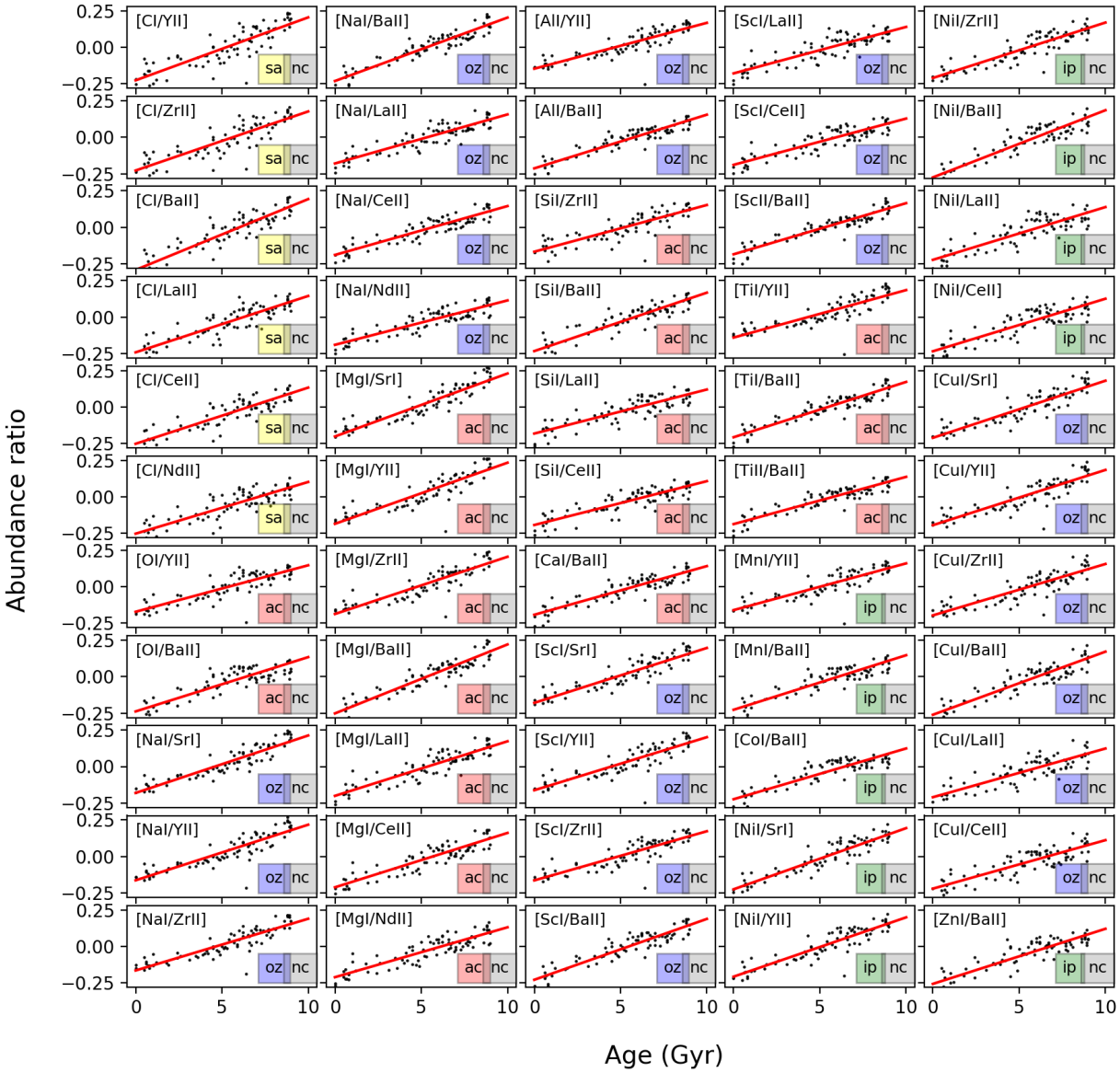

Fig. 1. Selected abundance ratios as a function of age in solar twins together with the linear fits of the trends. The abundance ratio is indicated in the top left corner of all panels, and the nucleosynthetic family of each abundance in a different colour in the bottom right corner (see Table 2 for the definition of each label).

Table 2. Nucleosynthetic families of elements.

Family	Label	Elements
Carbon	sa	C
α-capture	ac	O, Mg, Si, S, Ca, Ti
odd-Z	oz	Na, Al, Cu, Sc, V
iron-peak	ip	Cr, Mn, Fe, Co, Ni, Zn
n-capture	nc	Sr, Y, Zr, Ba, La, Ce Pr, Nd, Sm, Eu, Gd, Dy

Notes. The label is used as reference in Fig. 1.

populations. This ratio is negative for halo stars and zero for disc stars, which suggests that the carbon s-process contribution plays an important role as metallicity increases. This contradicts our reasoning that slopes in trends of abundance ratios with age increase when the production sites for the elements differ. Our sample contains stars of the same metallicity but different ages, however. Limongi & Chieffi (2018) presented an extensive nucleosynthesis study of massive stars and obtained that the relative production of C with respect to O increases with metallicity. The large slopes of C with respect to several s-process elements found here offer new alternatives for studying the production mechanisms of this element.

The relation of the odd-Z element Al with respect to Y has also caught the attention in the literature (Nissen 2016). It is explained following similar nucleosynthetic arguments as for [Mg/Y], that the rapid production of Al in core-collapse SNe of massive stars is compensated for by the increasing contribution of Y from lower mass AGB stars in time. Na is produced in a similar way as Al; these are alternatives to stellar population studies (Hawkins et al. 2015). Nissen (2016) further discussed that [Cu/Na] remains constant over time and suggested a similar production site for these elements. Our traits for the odd-Z family contain both Cu and Na elements with respect to similar n-capture elements.

Table 3. Mean slopes and their standard deviation for traits separated by *n*-capture element or by family.

Element family	Number	Mean slope (dex Gyr^{-1})	Std. dev (dex Gyr^{-1})
Ba	16	0.039	0.005
Ce	7	0.034	0.003
La	7	0.034	0.003
Nd	3	0.033	0.002
Sr	5	0.040	0.002
Y	10	0.037	0.004
Zr	7	0.036	0.003
ac	17	0.036	0.005
ip	10	0.038	0.004
oz	22	0.036	0.004
sa	6	0.041	0.004

Notes. The number column indicates how often this particular element or family was selected.

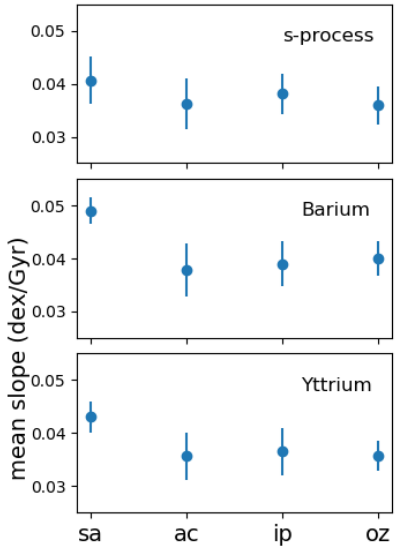

Fig. 2. Mean and standard deviations of slopes grouped by their families. The *first panel* corresponds to all selected *n*-capture elements, and the *second and third panels* consider only the results for Ba and Y, respectively.

Ni seems to be the iron-peak element with the strongest influence, which could be explained by the strong [Na/Ni] correlation found for this type of stars (Nissen 2015) and the strong positive [Ni/Fe] correlation found by Bedell et al. (2018). It is interesting to note that while we set the threshold for selecting our traits higher than the typical slopes found for [X/Fe], we selected iron-peak elements. This means that the iron-peak family does not necessarily have a weaker dependence on age when its ratio with *s*-process abundances is considered (see Table 3). The iron-peak family has indeed a variety of mechanisms for creating elements, and is expelled to the interstellar medium by different supernovae. [Mn/Fe], for example, has significant trends as a function of [Fe/H], and Zn is also abundantly produced by very massive stars (Kobayashi et al. 2006).

5. Conclusion

We presented the results of abundance ratios as a function of stellar ages for a set of 80 solar twins, for which 30 different chemical elements were measured with high precision by Bedell et al. (2018, and references therein). By selecting only the trends whose linear fit yielded a correlation factor above 70% and a slope above 0.03 dex Gyr^{-1}, we found 55 abundance ratios, including the widely discussed [Mg/Y] and [Mg/Ba] "chemical clocks".

All of them included two different nucleosynthetic families, and all included one *n*-capture element whose *s*-process percentage to the solar abundance is higher than the *r*-process percentage. The highest slope we found was for [C/Ba] of $\sim 0.05 \pm 0.003$ dex Gyr^{-1}. No abundance ratio appears to evolve faster than ~ 0.05 dex Gyr^{-1} in solar twins.

The new era of industrial stellar abundances from on-going and future spectroscopic surveys has just begun and already provides the community with datasets of chemical abundances of elements in all families considered here (Jofré et al. 2019). In particular, based on *Gaia* and seismic missions such as *Kepler* or TESS, it is becoming possible to estimate age distributions of many stars in the Milky Way. Investigating how the traits for chemical evolution found here behave in different conditions can provide new insights for constraining the chemodynamical models of the formation and evolution of our Galaxy. Much of this information is already available. We should take the opportunity to explore it by considering abundance ratios as a function the *s*-process elements.

Acknowledgements. We thank the referee for their positive and thoughtful comments, which helped to significantly order the discussions. We warmly acknowledge K. Yaxley, D. Boubert and P. Das for lively discussions on evolution of traits in general. We further acknowledge support from the MIT International Science and Technology Initiatives (MISTI) grant, which funded H. J. research visit from which these results were obtained. P. J. is partially funded by FONDECYT Iniciación grant Number 11170174. M. T. and P. J. thank the Joint Committee ESO-Chile for postdoctoral financial support, and ECOS-Conicyt for enabling travel and relevant discussions that lead to this Letter.

References

Aguilera-Gómez, C., Ramírez, I., & Chanamé, J. 2018, A&A, 614, A55
Amarsi, A. M., Nissen, P. E., & Skúladóttir, Á. 2019, A&A, 630, A104
Battistini, C., & Bensby, T. 2016, A&A, 586, A49
Bedell, M., Bean, J. L., Meléndez, J., et al. 2018, ApJ, 865, 68
Bisterzo, S., Travaglio, C., Gallino, R., Wiescher, M., & Käppeler, F. 2014, ApJ, 787, 10
da Silva, R., Porto de Mello, G. F., Milone, A. C., et al. 2012, A&A, 542, A84
Delgado Mena, E., Moya, A., Adibekyan, V., et al. 2019, A&A, 624, A78
Dotter, A., Conroy, C., Cargile, P., & Asplund, M. 2017, ApJ, 840, 99
Feltzing, S., Howes, L. M., McMillan, P. J., & Stonkutė, E. 2017, MNRAS, 465, L109
Feuillet, D. K., Bovy, J., Holtzman, J., et al. 2018, MNRAS, 477, 2326
Freeman, K., & Bland-Hawthorn, J. 2002, ARA&A, 40, 487
Hawkins, K., Jofré, P., Masseron, T., & Gilmore, G. 2015, MNRAS, 453, 758
Jofré, P., Das, P., Bertranpetit, J., & Foley, R. 2017, MNRAS, 467, 1140
Jofré, P., Heiter, U., & Soubiran, C. 2019, ARA&A, 57, 571
Karakas, A. I., & Lugaro, M. 2016, ApJ, 825, 26
Kobayashi, C., Umeda, H., Nomoto, K., Tominaga, N., & Ohkubo, T. 2006, ApJ, 653, 1145
Limongi, M., & Chieffi, A. 2018, ApJS, 237, 13
Masseron, T., Lagarde, N., Miglio, A., Elsworth, Y., & Gilmore, G. 2017, MNRAS, 464, 3021
Meléndez, J., Asplund, M., Gustafsson, B., & Yong, D. 2009, ApJ, 704, L66
Nissen, P. E. 2015, A&A, 579, A52
Nissen, P. E. 2016, A&A, 593, A65
Nomoto, K., Kobayashi, C., & Tominaga, N. 2013, ARA&A, 51, 457
Skúladóttir, Á., Hansen, C. J., Salvadori, S., & Choplin, A. 2019, A&A, 631, A171
Slumstrup, D., Grundahl, F., Brogaard, K., et al. 2017, A&A, 604, L8
Spina, L., Meléndez, J., Karakas, A. I., et al. 2016, A&A, 593, A125
Spina, L., Meléndez, J., Karakas, A. I., et al. 2018, MNRAS, 474, 2580
Tucci Maia, M., Ramírez, I., Meléndez, J., et al. 2016, A&A, 590, A32
Tucci Maia, M., Meléndez, J., Lorenzo-Oliveira, D., Spina, L., & Jofré, P. 2019, A&A, 628, A126